Received: 12 September 2023 | Revised: 1 November 2023 | Accepted: 5 December 2023

DOI: 10.1002/ces2.10199

International Journal of Ceramic Engineering & Science

RESEARCH ARTICLE

Nanofatigue of supercrystalline nanocomposites

Cong Yan[1] | **Diletta Giuntini**[1,2]

[1]Department of Mechanical Engineering, Eindhoven University of Technology, Eindhoven, The Netherlands

[2]Institute of Advanced Ceramics, Hamburg University of Technology, Hamburg, Germany

Correspondence
Diletta Giuntini, Department of Mechanical Engineering, Eindhoven University of Technology, Eindhoven, The Netherlands.
Email: d.giuntini@tue.nl

Funding information
Deutsche Forschungsgemeinschaft, Grant/Award Number: GI 1471/1-1

Abstract

Supercrystalline nanocomposites (SCNCs) are a new category of hybrid materials consisting of inorganic nanoparticles surface-functionalized with organic ligands and with periodic nanostructures, featuring multi-functionality and able to reach exceptional mechanical properties. Although efforts have been made to explore their mechanical behavior, their response to cyclic loading remains to be unveiled. Here, the fatigue behavior of SCNCs with different degrees of organic crosslinking is investigated via nanoindentation. The nanocomposites' fatigue life is assessed, and it emerges that SCNCs without crosslinking are more efficient in dissipating energy under cyclic loading and thus feature a longer fatigue life. Chipping is identified as the main fatigue failure mechanism, whereas different mechanisms, intrinsic or extrinsic, dominate in the indentation depth propagation, again depending on crosslinking.

KEYWORDS
fatigue, nanocomposites, nanoindentation, supercrystals

1 | INTRODUCTION

Supercrystalline nanocomposites (SCNCs) are promising candidates as multifunctional hybrid materials that can achieve remarkable mechanical properties.[1] They consist of inorganic nanoparticles (NPs) that are surface-functionalized with organic ligands and arranged into periodic structures, analogous to those of atomic crystals. These structures are also termed "superlattices."[2] A broad spectrum of emergent properties can be fostered in SCNCs, thanks to the combination of their nanoscale building blocks and arrangement in superlattices, leading to promising applications in battery electrodes, catalysts, optoelectronic, and magnetic devices.[2–4]

However, the mechanical behavior of SCNCs remains poorly understood. Current studies focus on their elastic modulus and hardness, whereas fewer address aspects of strength and fracture toughness.[5–13] Their time-dependent behavior, instead, is just starting to be assessed, and so far in terms of creep, that is, long-term deformation under static or quasi-static load.[14] A completely unexplored aspect is their response to cyclic loads, that is, their fatigue behavior, which is, nevertheless, a prominent cause of material failure,[15] especially considering that SCNCs in the applications listed above will be subjected to oscillating thermomechanical loads. It has become clear that the NP-functionalizing organic ligands play a key role in tuning mechanical properties and deformation behavior of SCNCs,[10,16] but their influence on fatigue has remained unaddressed. Considering the ligands' unique state and conformation—anchored to the NPs, ultra-confined in sub-nm spacings, and sometimes crosslinked[11]—elucidating their role in the context of

SCNCs will also shed light for a broader category of hybrid nanomaterials.

Although SCNCs can be upscaled to components with sizes in the centimeter range, especially when used as building blocks in hierarchical composites,[17–19] purely supercrystalline materials still pose challenges for macroscopic testing, due to pores and cracks arising during processing.[5] Conventional fatigue tests also entail lengthy and relatively complex sample preparation procedures. As a viable alternative, instrumented indentation has proven to be a valuable platform for small volume and local property measurement, progressively becoming a reliable, robust, and well-documented testing technique.[20] Indentation fatigue tests can be conducted under either multi-loading/unloading cycles or continuous stiffness measurement (CSM) mode,[21–24] in which an adjustable harmonic load is superimposed to the static one,[25] a method that has been successfully applied, for example, in thin films, coatings, ceramics, and core–shell nanostructures.[24,26–30] Even though the loading scheme, stress state, and indented volume differ between conventional fatigue and indentation fatigue tests,[15] indentation fatigue models have been proposed and validated, allowing access to data on indentation fatigue strength[31] and indentation depth propagation laws,[32] making indentation fatigue testing particularly attractive for small domains and nanostructured materials.

Here, the nanofatigue behavior of ceramic-based SCNCs is characterized by nanoindentation under CSM mode. The fatigue life is evaluated for materials featuring varying degrees of ligands' crosslinking. Ligand crosslinking is known to significantly boost the mechanical properties of SCNCs,[11,33] and to play a role on altering their deformability.[16] The—at times surprising—data is rationalized by assessing the nanocomposites' loss factor and thus their potential to dissipate energy under cyclic loading. The indentation depth propagation law is critically assessed for applicability to SCNCs, to identify the governing material deformation mechanisms in fatigue conditions. The interactions among the organic ligands result to be controlling the nanofatigue behavior of SCNCs.

2 | MATERIALS AND METHODS

The SCNCs studied here as model materials consist of iron oxide (Fe_3O_4) NPs surface-functionalized with oleic acid. Their fabrication follows a procedure detailed elsewhere[14] and is summarized in Section S1. Three samples with varying degrees of organic ligands' crosslinking were prepared for nanofatigue tests. These are termed as-pressed (AP, i.e., without the application of any heat treatment), heat-treated at 250°C (HT250) and at 325°C (HT325), and

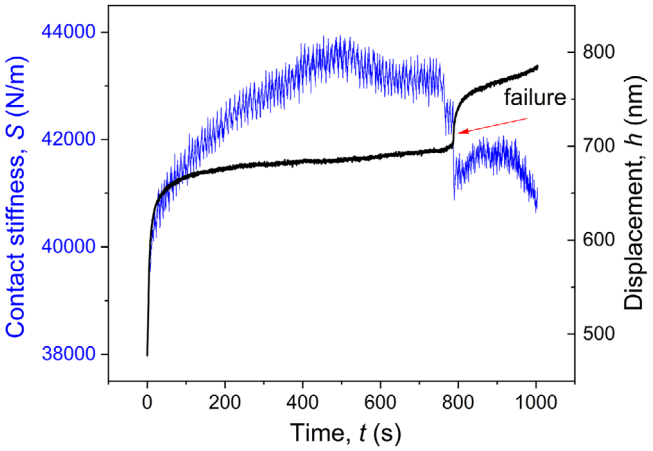

FIGURE 1 Identification of nanofatigue failure event as abrupt drop of contact stiffness. Correspondingly, the displacement data also exhibits a sharp increase at the onset of the fatigue failure.

they feature increasing levels of crosslinking. Crosslinking alters the conformation and interactions among adjacent organic ligands in the sub-nm space between NPs. From the "rearrangeable" organic chains mainly interacting via van der Waals forces in AP SCNCs, we shift to an interconnected covalent network in HT325 SCNCs. Partial decomposition of the ligands also occurs, typically leading to smaller interparticle distances in heat-treated materials. All details on the crosslinking process have been elucidated.[33] The nanofatigue tests were carried out in a G200 nanoindenter (Agilent) at room temperature, with a spherical tip. The tip has a nominal radius of 1 μm, calibrated to be 947 nm. The load first ramps up to a mean value under single-loading mode and at a loading rate of 0.2 mN/s, to avoid the effect of oscillations. Subsequently, the mode switches to CSM to enable the application of a cyclic load, with a frequency of 100 Hz. This process lasts for 1000 s, corresponding to 10^5 cycles. The load ratio (minimum load/maximum load) is kept as 0.1 for all nanofatigue tests. The mean loads and the corresponding load amplitudes are listed in Table 1. Mean load and load amplitude are higher for AP samples, because no or very few nanofatigue failure events were detected in this material until the load amplitude was increased to 1.485 mN; see Figure S1. Nanofatigue failure is identified as a sudden change of contact stiffness, thanks to the sensitivity of this parameter to damage,[34] as illustrated in Figure 1. At least 15 indents were performed for each load, with a spacing of 30 μm. The indents were observed via a scanning electron microscope (Zeiss 55-VP, Zeiss) at 2 kV to check their morphologies and failure mechanisms. Topographic measurements were also conducted via an atomic force microscope (NanoScope IV, Dimension 3100 of Digital Instruments), with a scanning speed of 0.5 Hz.

TABLE 1 Mean load and corresponding load amplitude of the performed nanofatigue tests.

HT250 & HT325	Mean load (mN)	0.99	1.10	1.12	1.21	1.32		1.87		2.04
	Load amplitude (mN)	0.81	0.90	0.95	0.99	1.08		1.53		1.67
AP	Mean load (mN)						1.82	1.87	1.98	2.04	2.09
	Load amplitude (mN)						1.49	1.53	1.62	1.67	1.71

Abbreviations: AP, as-pressed; HT250, heat-treated at 250°C; HT325, heat-treated at 325°C.

3 | RESULTS AND DISCUSSION

For uniaxial fatigue tests, the relationship between stress amplitude and number of cycles to failure can be quantitatively described by the conventional fatigue strength law, in the form of *S*–*N* curves. Inspired by this law and the analogy between conventional fatigue and indentation fatigue tests, Xu et al. proposed a similar law to correlate their relationship in indentation fatigue tests[31]:

$$F_a = F_f \left(N_f\right)^k \tag{1}$$

where F_a is the load amplitude and N_f is the number of cycles to failure; F_f and k are indentation fatigue strength coefficient and exponent, respectively, depending on the material and testing conditions. This model has been successfully applied to different materials, such as bulk PVC, TiN/NiP films,[31] and high entropy alloys in both film and bulk form.[24] Here, it is applied to SCNCs, as shown in Figure 2A. A linear relationship between load amplitude and number of cycles to failure is observed for the three different materials. Interestingly, AP SCNCs possess the longest fatigue life, followed by HT325, whereas HT250—the intermediate-crosslinking case—has the shortest one. This trend stands out, as typically the resistance of SCNCs to mechanical loading increases with an increasing degree of crosslinking.

The indentation fatigue strength coefficient (F_f), identified via the fitting intercept, is associated with static fracture strength.[31] The smallest value of F_f obtained for AP materials is consistent with their lower fracture strength,[5,35] whereas F_f is the highest for the SCNCs with the largest degree of crosslinking. The indentation fatigue strength exponent (k), determined as the fitting slope, can instead shed light on the materials' sensitivity to damage: The steeper the slope, the more sensitive to damage the material is, and the earlier failure occurs. AP materials have a relatively flat fitting line, with longer overall fatigue life, whereas the opposite trend is observed for heat-treated samples. No obvious difference is observed between HT250 and HT325 SCNCs with respect to the slopes of *F*–*N* curves. As the heat treatment effect on the degree of crosslinking and overall ligand decomposition cannot be quantified, the value of k cannot be directly correlated with one of these factors, which both contribute to the materials' sensitivity to damage. The analysis of the *F*–*N* curves confirms then the applicability of indentation fatigue strength models to SCNCs but also reveals unexpected fatigue properties of nanocomposites with varying degrees of crosslinking.

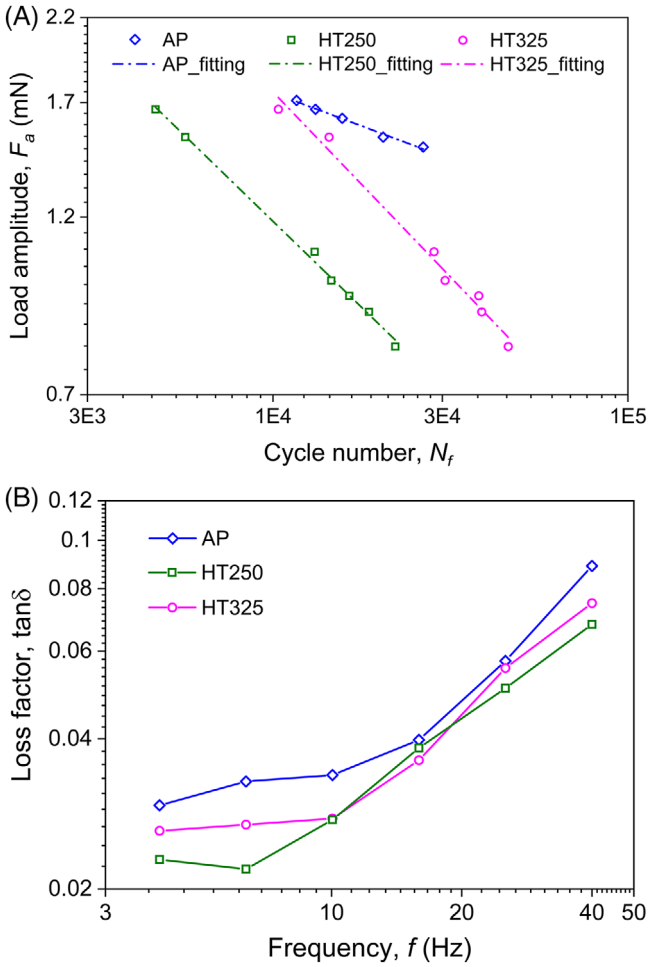

FIGURE 2 Fatigue life and loss factors of supercrystalline nanocomposites (SCNCs) with varying degrees of crosslinking: (A) Relationship between load amplitude (F_a) and number of cycles to failure (N_f) in double logarithmic plot. The dashed lines denote the fitting based on Equation (1), obtained with a high correlation coefficient ($R^2 > 0.95$). (B) Variation of loss factor (ratio of loss modulus to storage modulus) with respect to frequency.

To understand the reasons lying behind the different fatigue lives, dynamic nanoindentation tests were carried

out to obtain each material's loss factor, which is an indicator of the material's potential to dissipate energy,[36,37] as displayed in Figure 2B. The tests were performed under CSM mode, with a harmonic displacement of 3 nm and frequency ranging from 4 to 40 Hz, and with a 10 μm-diameter flat punch. The AP SCNCs consistently show the highest loss factor across the varying frequencies, the HT250 ones show the lowest one, whereas intermediate values are recorded for HT325 materials (with a small exception at 15.9 Hz). This trend in loss factors is consistent with the fatigue lives in Figure 2A. Due to limitations of the nanoindentation system, the frequency during dynamic nanoindentation tests cannot be extended to 100 Hz, and therefore, here it is assumed that the trend of Figure 2B is preserved at higher frequencies. The measured SCNCs' loss factors are lower than those of polymers (~1 order of magnitude),[38] but comparable to those of cluster-assembled solids.[36]

The results displayed in Figure 2 demonstrate that the nanocomposites' capability to dissipate energy plays a dominating role in their fatigue life. This can be explained by considering the interactions between ligands in the absence or presence of crosslinking. The ceramic NPs in AP materials are held together mainly by van der Waals forces, as no or negligible crosslinking is induced among the ligands.[5] Consequently, the ligands in the inter-NP spacings can easily bend or deform during loading and recover during unloading, effectively dissipating energy at each applied load cycle. On the other hand, heat treatment induces crosslinking, that is, the formation of covalent bonds within the organic phase, resulting in a strongly interconnected ligand network replacing the rearrangeable organic chains,[5] together with the partial decomposition of the ligands.[33] The bending and recovery of ligands become thus significantly restricted, weakening the crosslinked SCNCs' ability to dissipate energy, and therefore resulting in a shorter fatigue life for the heat-treated nanocomposites.

The different fatigue lives of HT250 and HT325 nanocomposites, with HT250 SCNCs showing lower resistance against fatigue, can be further understood from the viewpoint of crack initiation and propagation. The AP materials are most prone to crack initiation, due to their lower fracture toughness compared to the case of HT325 SCNCs,[11,35] whereas at the same time, AP nanocomposites exhibit a better ability to dissipate energy due to the higher flexibility of the ligands. HT250 SCNCs have crosslinking, even though at a lower level compared to HT325 ones, and they can thus be seen as an intermediate case between AP and HT325 nanocomposites: They are less resistant to crack initiation than HT325 supercrystals, and they have lost some of their ability to dissipate energy under cyclic load compared to the AP case.

The typical indents' morphologies after the nanofatigue test are shown in Figure 3. Chipping is induced in AP SCNCs (Figure 3A). The same feature, even though less severe, is found in HT250 SCNCs (Figure 3B), accompanied by a ring crack (indicated by the arrow). In Figure 3C, small supercrystalline fragments, also likely associated with chipping, are accumulated around an indent in HT325 SCNCs. Chipping then appears to be the main failure mechanism in SCNCs both with and without crosslinking, a phenomenon also reported for indentation fatigue of brittle materials.[30] Chipping is attributed to lateral cracking, initiated during unloading cycles as a result of tensile stresses.[30]

Interestingly, there are some indents that show no nanofatigue failure during the entire 10^5 cycles. The main deformation features in these cases are relatively uniform pileups around the indents; see Figure S2. The height of the pileups was measured to be ~150 nm for AP, 50 nm for HT250, and 30 nm for HT325 SCNCs, in-line with the strengthening effect of crosslinking. Even in presence of these pileups, slight chipping can still be observed in AP and HT250 materials, likely formed during the unloading segment (after application of the cyclic load). This interesting phenomenon may be related to the orientation of supercrystalline domains or local heterogeneities of the nanocomposites' constituents, and it thus requires further investigation.

Another important aspect to analyze to better grasp the fatigue behavior of SCNCs is the depth propagation law. The tip can continuously sink into the samples under indentation fatigue tests, leading to a quick sinking in a transition stage, followed by a leveling-off depth propagation rate in a steady-state regime. This process is very reminiscent of crack propagation in conventional fatigue tests.[32,39,40] For ductile materials, indentation depth propagation can be ascribed to the advancement of the plastic zone under the indent, whereas for brittle materials, it is usually caused by the propagation of damaged zone facilitated by microcracks.[30,39,41] The analogy between uniaxial fatigue and indentation fatigue tests has been explored, resulting in a model aimed at elucidating governing mechanisms (intrinsic/extrinsic) in indentation depth propagation.[32] Indentation fatigue and conventional fatigue share the feature of showing a stress singularity, which in indentation lies at the rim of the contact with the indenting punch, analogous to a crack tip.[42] A cone crack can be initiated from the contact edge, where the largest tensile stress is located,[43] either when loading with a spherical tip or a flat punch.[44] As no significant difference is found in terms of cone crack extension direction between flat punch and spherical tip indentation,[44] the indentation depth propagation model can be extended to the case of spherical tip.

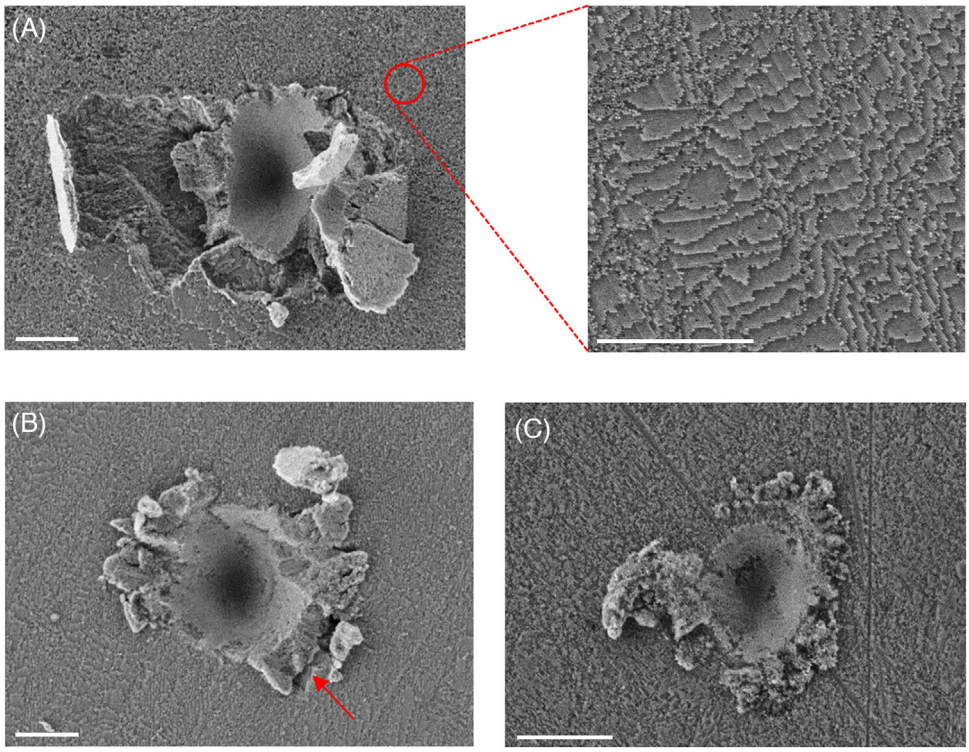

FIGURE 3 Morphologies of indents after fatigue failure, obtained with a load amplitude of 1.53 mN for as-pressed (AP), 0.95 mN for heat-treated at 250°C (HT250) and HT at 325°C (HT325) supercrystalline nanocomposites (SCNCs): (A) chipping around indent in AP SCNC, with a magnification of the supercrystalline nanostructure; (B) HT250 SCNC; (C) HT325 SCNC. Scale bars are 1 μm.

The indentation depth propagation tests were carried out with a load ratio of 0.2, to delay fatigue failure. Three different pairs of mean load and load amplitude were selected: 1.2 ± 0.8, 1.5 ± 1, and 1.8 ± 1.2 mN, with all other parameters kept unchanged from nanofatigue tests. Again, failure occurred first in HT250 SCNCs (here in 6 indents out of 10 under 1.5 ± 1 mN cyclic loading), in line with the outcomes of the *F*–*N* analyses, and thus in the following only the results relative to AP and HT325 SCNCs are shown. The indentation depth propagation under 1.5 ± 1 mN is shown in Figure 4A, together with the corresponding propagation rates in Figure 4B, both of which feature a quick sinking in the beginning, followed by a slowdown until a quasi-steady state, analogous to the first two stages of fatigue crack propagation. The same trend is observed in the case of 1.2 ± 0.8 and 1.8 ± 1.2 mN, as shown in Figure S3.

The indentation depth propagation model[45] that enables identifying the underlying mechanisms is then applied:

$$\left(\frac{\mathrm{d}d}{\mathrm{d}N}\right)_s = C(K_{\max})^m(\Delta K)^n \tag{2}$$

where dd/dN is the depth propagation rate in the steady state (as the subscript "s" indicates); C, m, and n are constants depending on material and testing conditions.[32] The maximum stress intensity factor $K_{\max}$ and stress intensity factor range ΔK can be computed as

$$K_{\max} = \frac{P_{\max}}{2a\sqrt{\pi a}} \tag{3}$$

$$\Delta K = \frac{\Delta P}{2a\sqrt{\pi a}} \tag{4}$$

where a is contact radius; $P_{\max}$ and ΔP are maximum load and load range, respectively.[32] The contact radius is calculated as $a = \sqrt{2Rh_c - h_c^2}$, where R is the radius of spherical tip, and h_c is contact depth. The contact depth is obtained as

$$h_c = h - \frac{\varepsilon P}{S} \tag{5}$$

where h is the measured displacement and S is the contact stiffness, whereas $\varepsilon = 0.75$ for spherical tips.[46] The two exponents, m and n, associated with extrinsic or intrinsic mechanism responsible for the indentation depth propagation, can be obtained by regression analysis via Equation (2), where the Levenberg–Marquardt algorithm is adopted and yields a very high correlation coefficient ($R^2 > 99\%$). The propagation rate (dd/dN) is estimated after 6×10^4 cycles, that is, in quasi-steady state, as marked in Figure 4B. Their values under different mean loads and

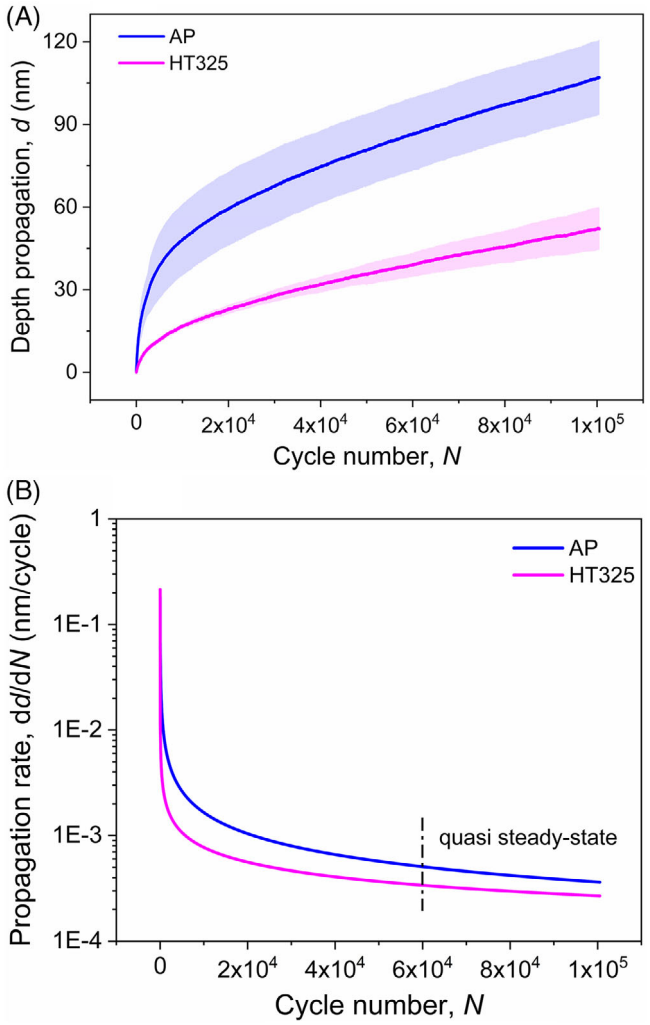

FIGURE 4 Nanoindentation depth propagation tests under 1.5 ± 1 mN cyclic loading: (A) depth propagation and (B) corresponding propagation rate. The shaded bands in (A) denote the standard deviation.

TABLE 2 Summary of m and n under different mean loads and load amplitudes.

Mean load ± load amplitude (mN)	AP		HT325	
	m	n	m	n
1.2 ± 0.8	9.0	7.9	2.3	3.2
1.5 ± 1.0	7.3	4.8	2.2	3.1
1.8 ± 1.2	10.2	6.9	4.0	5.7

Abbreviations: AP, as-pressed; HT325, heat-treated at 325°C.

load amplitudes are displayed in Table 2, and the respective averages are determined as $m = 8.8$ and $n = 6.5$ for AP SCNCs, and $m = 2.8$ and $n = 4.0$ for HT325 SCNCs.

The propagation rate ($\mathrm{d}d/\mathrm{d}N$), then, has a stronger dependence on $K_{\max}$ ($m > n$) in AP SCNCs, whereas on ΔK ($m < n$) for HT325 ones. The growth of fatigue cracks can be seen as a mutual competition between intrinsic mechanisms of crack advancement ahead of the crack tip, dependent on ΔK as the driving force of crack propagation, and extrinsic mechanisms of crack-tip shielding behind the tip, controlled by $K_{\max}$.[45] These competing crack growth mechanisms can be correlated to the indentation depth propagation.[32,47] Extrinsic mechanisms thus dominate in the depth propagation for AP SCNCs, whereas intrinsic mechanisms are predominant in HT325 ones.

The interactions among NPs need to be again considered to explain this substantial difference. As van der Waals interactions dominate in AP materials,[5] whereby intact oleic acid chains, uncrosslinked, at the NP interfaces play a major role in allowing plastic deformation of the superlattices,[16] NPs can easily be rearranged under cyclic loading, resulting in the formation of micro-plastic zones, relieving the applied stress. At the same time, energy can also be partially dissipated by non-crosslinked ligands. The driving force for depth propagation is thus diminished, decelerating the process, hinting at extrinsic mechanism in AP materials. In HT325 SCNCs, the mechanical properties are enhanced thanks to crosslinking,[11,33] and stress relief becomes less efficient due to the difficult rearrangement of NPs, leading to the dominance of intrinsic mechanisms. It is also very likely that indentation depth propagation in SCNCs is accompanied by microcracks, due to the non-pronounced plasticity of SCNCs, although no catastrophic failure (crack or chipping) is observed.

4 | CONCLUSIONS

The nanofatigue tests of ceramic-based SCNCs with different degrees of crosslinking were carried out thanks to CSM mode in nanoindenter. AP SCNCs thus possess the longest fatigue life, followed by HT325, whereas HT250 SCNCs have the shortest one, as explained by their respective loss factors, characterizing the potential to dissipate energy. Chipping is identified as the major failure mechanism, whereas the governing factors in nanoindentation depth propagation result to be dominatingly extrinsic in AP SCNCs and intrinsic in the case of HT325. Although ligands only occupy a minor fraction of SCNCs, this study reveals their strong influence on the nanocomposites' dynamic mechanical behavior, tuneable by ligand crosslinking. Other approaches to tailor fatigue properties of SCNCs can be identified in controlling the ligands' density and their molecular length, paving the way toward an ever-broader spectrum of applications for this new category of hybrid materials.

ACKNOWLEDGMENTS

The authors gratefully acknowledge the financial support from the Deutsche Forschungsgemeinschaft (DFG,

German Research Foundation), project number GI 1471/1-1. The authors are thankful to Dr. Jasmin Koldehoff (Hamburg University of Technology) for the assistance with nanoindentation tests and Dr. Alexander Plunkett (Hamburg University of Technology) for the assistance with sample preparation.

ORCID

Cong Yan https://orcid.org/0000-0003-4359-9802

REFERENCES

1. Begley MR, Gianola DS, Ray TR. Bridging functional nanocomposites to robust macroscale devices. Science. 2019;364:eaav4299.
2. Boles MA, Engel M, Talapin DV. Self-assembly of colloidal nanocrystals: from intricate structures to functional materials. Chem Rev. 2016;116:11220–89.
3. Sturm EV, Cölfen H. Mesocrystals: past, presence, future.Crystals. 2017;7:207.
4. Pileni MP. Nanocrystal self-assemblies: fabrication and collective properties. J Phys Chem B. 2001;105:3358–71.
5. Dreyer A, Feld A, Kornowski A, Yilmaz ED, Noei H, Meyer A, et al. Organically linked iron oxide nanoparticle supercrystals with exceptional isotropic mechanical properties. Nat Mater. 2016;15:522–28.
6. Tam E, Podsiadlo P, Shevchenko E, Ogletree DF, Delplancke-Ogletree MP, Ashby PD. Mechanical properties of face-centered cubic supercrystals of nanocrystals. Nano Lett. 2010;10:2363–67.
7. Pileni MP. Mechanical properties of supracrystals. EPL. 2017;119:37002.
8. Gu XW. Mechanical properties of architected nanomaterials made from organic–inorganic nanocrystals. JOM. 2018;70:2205–17.
9. Podsiadlo P, Krylova G, Lee B, Critchley K, Gosztola DJ, Talapin Dv, et al. The role of order, nanocrystal size, and capping ligands in the collective mechanical response of three-dimensional nanocrystal solids. J Am Chem Soc. 2010;132:8953–60.
10. Domènech B, Plunkett A, Kampferbeck M, Blankenburg M, Bor B, Giuntini D, et al. Modulating the mechanical properties of supercrystalline nanocomposite materials via solvent-ligand interactions. Langmuir. 2019;35:13893–903.
11. Bor B, Giuntini D, Domènech B, Plunkett A, Kampferbeck M, Vossmeyer T, et al. Constitutive and fracture behavior of ultra-strong supercrystalline nanocomposites. Appl Phys Rev. 2021;8:031414.
12. Yan C, Bor B, Plunkett A, Domènech B, Schneider GA, Giuntini D. Nanoindentation of supercrystalline nanocomposites: linear relationship between elastic modulus and hardness. JOM. 2022;74:2261–76.
13. Giuntini D, Torresani E, Chan KT, Blankenburg M, Saviot L, Bor B, et al. Iron oxide-based nanostructured ceramics with tailored magnetic and mechanical properties: development of mechanically robust, bulk superparamagnetic materials. Nanoscale Adv. 2019;1:3139–50.
14. Yan C, Bor B, Plunkett A, Domènech B, Maier-Kiener V, Giuntini D. Nanoindentation creep of supercrystalline nanocomposites. Mater Des. 2023;231:112000.
15. Islam MM, Shakil SI, Shaheen NM, Bayati P, Haghshenas M. An overview of microscale indentation fatigue: composites, thin films, coatings, and ceramics. Micron. 2021;7:103110.
16. Giuntini D, Zhao S, Krekeler T, Li M, Blankenburg M, Bor B, et al. Defects and plasticity in ultrastrong supercrystalline nanocomposites. Sci Adv. 2021;7:eabb6063.
17. Plunkett A, Warren KTC, Wisniewski V, Fiedler B, Furlan KP, Garay J, et al. Bridging nanocrystals to robust, multifunctional, bulk materials through nature-inspired, hierarchical design. Mater Sci. 2022; https://doi.org/10.26434/chemrxiv-2022-mxtm4
18. Bor B, Heilmann L, Domènech B, Kampferbeck M, Vossmeyer T, Weller H, et al. Mapping the mechanical properties of hierarchical supercrystalline ceramic-organic nanocomposites. Molecules. 2020;25:4790.
19. Domènech B, Kampferbeck M, Larsson E, Krekeler T, Bor B, Giuntini D, et al. Hierarchical supercrystalline nanocomposites through the self-assembly of organically-modified ceramic nanoparticles. Sci Rep. 2019;9:3435.
20. Bhushan B. Depth-sensing nanoindentation measurement techniques and applications. Microsyst Technol. 2017;23:1595–649.
21. Jia YF, Xuan FZ. Anisotropic fatigue behavior of human enamel characterized by multi-cycling nanoindentation. J Mech Behav Biomed Mater. 2012;16:163–68.
22. Faisal NH, Prathuru AK, Goel S, Ahmed R, Droubi MG, Beake BD, et al. Cyclic nanoindentation and nano-impact fatigue mechanisms of functionally graded TiN/TiNi film. Shap Mem Superelasticity. 2017;3:149–67.
23. Li X, Bhushan B. Fatigue studies of nanoscale structures for MEMS/NEMS applications using nanoindentation techniques. Surf Coat Technol. 2003;163:521–26.
24. Wang Z, Wang C, Zhao YL, Kai JJ, Liu CT, Hsueh CH. Fatigue studies of CoCrFeMnNi high entropy alloy films using nanoindentation dynamic mechanical analyses. Surf Coat Technol. 2021;410:126927.
25. Pethica JB, Oliver WC. Tip surface interactions in STM and AFM. Phys Scr. 1987;19:61–66.
26. Steck JG, Fleming RA, Goss JA, Zou M. Deformation and fatigue resistance of Al/a-Si core–shell nanostructures subjected to cyclic nanoindentation. Appl Surf Sci. 2018;433:617–26.
27. Weikert T, Wartzack S, Baloglu MV, Willner K, Gabel S, Merle B, et al. Evaluation of the surface fatigue behavior of amorphous carbon coatings through cyclic nanoindentation. Surf Coat Technol. 2021;407:126769.
28. Wang Z, Wang C, Zhao YL, Hsu YC, Li CL, Kai JJ, et al. High hardness and fatigue resistance of CoCrFeMnNi high entropy alloy films with ultrahigh-density nanotwins. Int J Plast. 2020;131:102726.
29. Khlifi K, Barhoumi N, Dhiflaoui H, ben Cheikh Larbi A. Fatigue behaviour and mechanical properties of PVD CrSiN coating using cyclic nanoindentation. Tribol Mater, Surfaces Interfaces. 2021;15:252–57.
30. Takakura E, Horibe S. Fatigue damage in ceramic materials caused by repeated indentation. J Mater Sci. 1992;27:6151–58.
31. Xu B, Yonezu A, Chen X. An indentation fatigue strength law. Philos Mag Lett. 2010;90:313–22.
32. Xu B, Yue Z, Chen X. An indentation fatigue depth propagation law. Scr Mater. 2009;60:854–57.

33. Plunkett A, Kampferbeck M, Bor B, Sazama U, Krekeler T, Bekaert L, et al. Strengthening engineered nanocrystal three-dimensional superlattices via ligand conformation and reactivity. ACS Nano. 2022;16:11692–707.
34. Li X, Bhushan B. A review of nanoindentation continuous stiffness measurement technique and its applications. Mater Charact. 2002;48:11–36.
35. Bor B, Giuntini D, Domènech B, Swain MV, Schneider GA. Nanoindentation-based study of the mechanical behavior of bulk supercrystalline ceramic–organic nanocomposites. J Eur Ceram Soc. 2019;39:3247–56.
36. Sugi KS, Bandyopadhyay P, Bodiuzzaman M, Nag A, Hridya M, Dar WA, et al. Manifestation of structural differences of atomically precise cluster-assembled solids in their mechanical properties. Chem Mater. 2020;32:7973–84.
37. Huang J, Xu Y, Qi S, Zhou J, Shi W, Zhao T, et al. Ultra-high energy-dissipation elastomers by precisely tailoring the relaxation of confined polymer fluids. Nat Commun. 2021;12:3610.
38. Herbert EG, Oliver WC, Pharr GM. Nanoindentation and the dynamic characterization of viscoelastic solids. J Phys D Appl Phys. 2008;41:074021.
39. Xu BX, Yue ZF, Wang J. Indentation fatigue behaviour of polycrystalline copper. Mech Mater. 2007;39:1066–80.
40. Chu SNG, Li JC. Delayed retardation of overloading effects in impression fatigue. J Eng Mater Technol. 1980;102:337–40.
41. Li JCM. Impression creep and other localized tests. Mater Sci Eng A. 2002;322:23–42.
42. Giannakopoulos AE, Lindley TC, Suresh S. Aspects of equivalence between contact mechanics and fracture mechanics: theoretical connections and a life-prediction methodology for fretting-fatigue. Acta Mater. 1998;46:2955–68.
43. Zeng K, Bredert K, Rowcliffe DJ. The Hertzian stress field and formation of cone crack—I. Theoretical approach. Acta Metall Mater. 1992;40:2595–600.
44. Fett T, Rizzi G, Diegele E. Weight functions for cone cracks. Eng Fract Mech. 2004;71:2551–60.
45. Ritchie RO. Mechanisms of fatigue-crack propagation in ductile and brittle solids. Int J Fract. 1999;100:55–83.
46. Oliver WC, Pharr GM. An improved technique for determining hardness and elastic modulus using load and displacement sensing indentation experiments. J Mater Res. 1992;7:1564–83.
47. Jain S, Gokhale A, Jain J, Singh SS, Hariharan K. Fatigue behavior of aged and solution treated AZ61 Mg alloy at small length scale using nanoindentation. Mater Sci Eng A. 2017;684:652–59.

SUPPORTING INFORMATION

Additional supporting information can be found online in the Supporting Information section at the end of this article.

How to cite this article: Yan C, Giuntini D. Nanofatigue of supercrystalline nanocomposites. Int J Ceramic Eng Sci. 2024;6:e10199. https://doi.org/10.1002/ces2.10199